

Chapter 8

Micromachining

Alexander Horn, Ulrich Klug, Jan Düsing, Javier Gonzalez Moreno, Viktor Schütz, Oliver Suttmann, Ludger Overmeyer, Andreas Lenk and Bodo Wojakowski

Abstract Micromachining using ultra-short pulsed laser radiation can be used to manipulate matter without interacting with the surrounding matter. This ideal processing, called “cold ablation”, is attributed to picosecond and femtosecond laser radiation, and nowadays there are applications in some special industrial processes. But ultrafast laser radiation can also be used to heat matter very locally, allowing new processing strategies for welding or annealing. Starting from typical micromachining conditions, the limitations and scaling up techniques for industrial ultra-short material processing are presented. Significant examples of possible industrial applications using ultrafast laser micromachining are presented, elucidating the applicability of this unique radiation source.

8.1 Ultra-Short Laser Pulses and Their Way into Industrial Applications

The first experiments on the interaction of ultra-short laser pulses with matter revealed a new kind of laser ablation mechanism characterized by the almost complete absence of recast and heat affected zones. “Cold ablation” immediately sparked the idea of pushing the accuracy of laser material processing to a new dimension. Simultaneously with the invention of the post-amplified solid state Ti:Sapphire femtosecond laser, the new ablation mechanism quickly found its way

A. Horn · U. Klug (✉) · J. Düsing · J.G. Moreno · V. Schütz · O. Suttmann · L. Overmeyer
Laser Zentrum Hannover e.V, Hollerithallee 8, 30419 Hannover, Germany
e-mail: u.klug@lzh.de

L. Overmeyer
ITA, Leibniz Universität Hannover, An der Universität 2, 30823 Garbsen, Germany

A. Lenk
Continental Automotive GmbH, Ostring 7, 09212 Limbach-Oberfrohna, Germany

B. Wojakowski
ALLTEC GmbH, An der Trave 27-31, 23923 Selmsdorf, Germany

into other research groups that focused on new laser machining applications. Since then, the number of publications regarding the effect of ultra-short laser pulses on structure resolution and the machining of delicate and heat-sensitive materials has progressively increased [1, 3, 9]. Negative effects known from conventional laser processing with continuous or nanosecond-pulsed lasers, such as melt spilling, could be avoided by using ultra-short laser radiation. Material is mostly vaporized, and is deposited only as re-solidified, removable debris. From the beginning, microstructures generated by laser ablation using Ti:Sapphire systems have been of superior quality, compared to longer pulsed systems, and is thus technically highly interesting for the micro- and nanotechnology community (Fig. 8.1). However, only a very small number of micromachining applications could successfully meet the requirements for commercial exploitation. Particularly, the technical complexity and the achievable system parameters, such as average power and pulse repetition rates of the Ti:Sapphire systems in the 1–10 kHz–regime were a limiting factor for economically interesting medium- and large-scale production. This situation dramatically changed in the beginning of this century, when ultra-short pulse generation and amplification concepts based on new laser media such as Nd:YVO₄ and Yb:YAG emerged. Different laser concepts were applied, starting from the known rod to the fiber, disk or slab designs. The new developments quickly provided reliable laser sources with ultra-short pulse durations less than 10 ps at high average power levels of up to multiple 100 W and repetition rates up to the MHz regime. This new generation of high-repetitive, ultra-short pulsed lasers offers a good tradeoff between process quality and process speed, that in return will provide profitable, high-quality laser micromachining processes, including the non-academic end user market.

A new microstructuring quality resulting from laser ablation using ultra-short pulsed laser radiation is, apart from production aspects, important for industrial applications. These applications show a possible technological advance:

- Burr-free drilling, cutting and texturing, without post-processing
- Processing of heat-sensitive materials such as biopolymers (poly lactate), or NiFe-alloys with magnetic properties
- Real layer-by-layer ablation (2.5-D structures) for shaped holes and texturing
- Post-processing of prefabricated microstructures, such as trimming and repairing of sensors
- Use of sacrificial layers without bonding to the substrate
- Selective thin-film structuring for sensor applications
- Multi-photon processes like 2-photon polymerization, in-glass scribing, and in-glass structuring

In fact, combining the processes mentioned with high-repetition, ultra-short lasers is still a challenge for the system technology, for example high-velocity, high-precision focused beam positioning. In order to maintain high ablation quality with the beam sources in the range of several hundred watts, very fast scanning techniques in the range of several 100 m/s are necessary. Already, industrial applications demonstrate the power of ultra-short laser microstructuring.

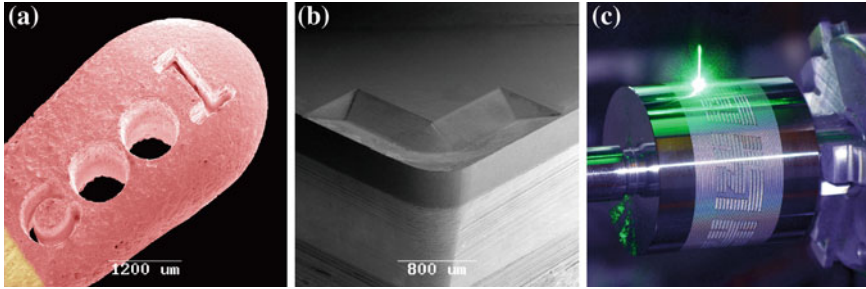
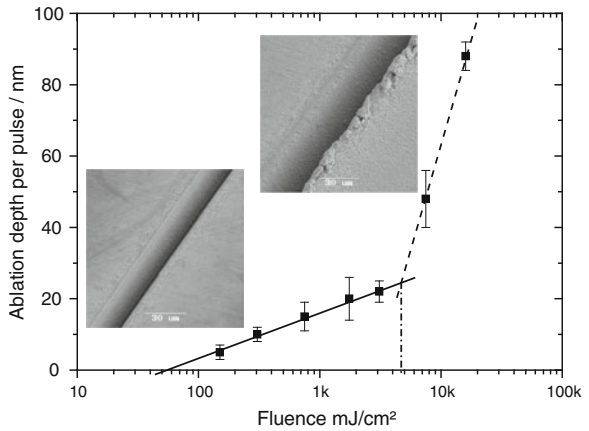


Fig. 8.1 a Laser drilled match tip, b laser structured chip breaker in polycrystalline diamond, c laser patterning of metallic cylinders

Fig. 8.2 Ablation depth per pulse for X20Cr13 versus incident laser fluence for 12-ps laser radiation. *Inlet* SEM of ablated grooves within the two regimes [15]



8.2 Residual Heat Due to Excessive Fluence

The characteristic ablation behavior with two ablation regimes [8] (Figs. 8.2 and 8.3) is typical for ultra-short laser processing. The ablation rate per pulse in dependence of the logarithmic fluence features a linear dependency. In this regime, also called the optical regime, single pulse ablation results in smooth surfaces, and for overlapping multi-pulses a periodic to quasi-periodic topology [10]. Above a transition fluence $F_{trans} > F_{thr}$, the linear dependency of the ablation rate continues, but with an increased slope (Fig. 8.2). Single pulse ablation is accompanied by melting, and multi-pulse ablation results in strong heating and melting of the substrates. Therefore, this regime is called the thermal regime (Fig. 8.2 and inlets).

The ablation depth for metals can be calculated by applying the two-temperature diffusion model, [8] and citations therein. One dimensionally, the temperature evolution of the electron and the lattice can be described by

$$C_e \frac{\partial T_e}{\partial t} = \frac{\partial Q(z)}{\partial z} - \gamma(T_e - T_i) + S \quad (8.1)$$

$$C_i \frac{\partial T_i}{\partial t} = \gamma(T_e - T_i) \quad (8.2)$$

$$Q(z) = -k_e \frac{\partial T_e}{\partial z} \quad (8.3)$$

$$S = I(t)A\alpha e^{-\alpha z} \quad (8.4)$$

where z is the direction perpendicular to the target surface, $Q(z)$ the heat flux, S the laser heating-source term, $I(t)$ the laser intensity, A and α the surface absorptivity and the material absorption coefficient, C_e and C_i the heat capacities (per unit volume) of the electron and lattice subsystems, γ the parameter characterizing the electron–lattice coupling, and k_e the electron thermal conductivity. In this simplified model following [8], one can calculate the ablation depth per pulse l being also driven by the optical penetration depth λ and thermal penetration depth δ :

$$l \propto \delta \ln \left(\frac{F_a}{F_{\text{thr}}^\delta} \right), \quad (\delta \gg \lambda) \quad (8.5)$$

$$l \propto \lambda \ln \left(\frac{F_a}{F_{\text{thr}}^\lambda} \right), \quad (\delta \ll \lambda) \quad (8.6)$$

The proportional factors detected for the ablation depth per pulse (Figs. 8.2 and 8.3) are represented by the optical or respectively thermal penetration depth. Precise microstructuring with smooth ablation features with little melt and small heat affect zones at fluencies below the transition fluence (inlet Fig. 8.3) are represented by an optical absorption behavior (8.5). Above the transition threshold, microstructuring is accompanied by re-solidified melt and large heat-affected zones.

8.3 Accumulated Heat Due to High Repetition Rates

The two-temperature model depicts ablation only in a semi-qualitative manner, and does not consider thermo- or hydrodynamics of the solid, the melt and the plasma. Also, a multi-dimensional approach will not sufficiently describe the observed heating due to high-repetitive, ultra-short laser radiation. In fact, apart from the vapor and the plasma plume interacting with the surface, excessive pulse energy not

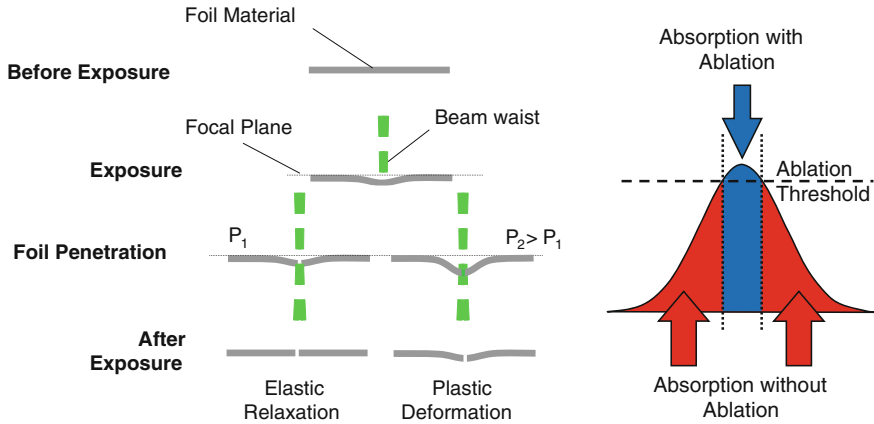


Fig. 8.3 Schematics on accumulated heat in percussion drilled foil material (*left*); description of the threshold definition and of accumulated heat (*right*)

contributing to ablation is partly converted to heat. At large repetition rates, the heat accumulates and the temperature rises within the interaction volume to values up to melting temperatures. This effect is disadvantageous for machining heat sensitive, microstructured materials (e.g. special alloys, ion-doped semiconductors, organics), but can also be used as a heat source, for example to weld glass [7].

Exemplary, drilling and cutting of thin sheets of metal, nylon or silicon using picosecond pulsed laser radiation [5] have been investigated. The thermally induced vertical displacement has been detected while drilling thin sheets irradiated at intensities above ablation threshold (Fig. 8.3 left).

By irradiating a metallic surface with focused Gaussian distributed laser radiation at fluencies above ablation threshold, two regions are characterized, see Fig. 8.3 right: the region within the dashed lines represents the ablated region, and the region outside the dashed lines represents the heated region. Multi-pulse irradiation of the metal surface results in an accumulation of heat followed by mechanical expansion of the material (Fig. 8.3 left). Depending on the thermo-mechanical material properties, a linear or nonlinear displacement is observed: For example, when irradiating thin foils of silicon with 50 μm thickness at a constant fluence, a linear dependence of the vertical displacement on increasing repetition rate is observed (Fig. 8.4 left), whereas steel and nylon depict a nonlinear one. Also, exposing the investigated material to laser radiation at a constant average power, but altering the repetition rate shows an increasing foil bending for steel foils, due to an increasing heat accumulation, though the fluence is decreasing. Applying high-repetitive, ultra-short laser radiation e.g. for high-density drilling thin sheets, need a drilling strategy, like ablating with a chaotic strategy reducing the local heat load. Or, the repetition rate must be reduced below 100 kHz, until the displacement is smaller than the precision needed (Fig. 8.4 right).

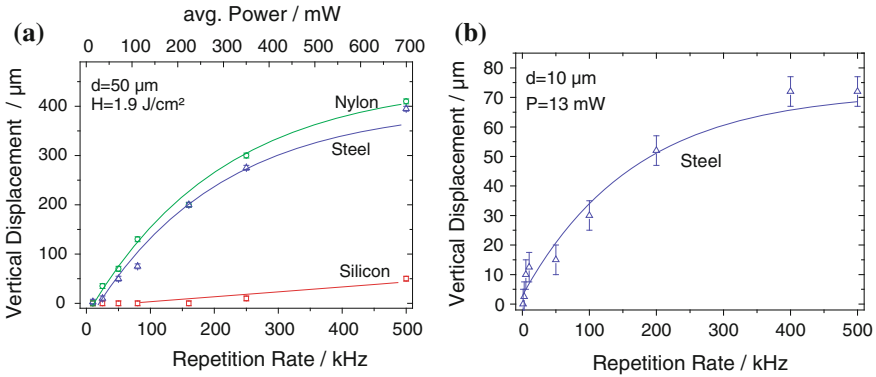


Fig. 8.4 **a** Displacement of 50 μm foil substrates versus average power. **b** Displacement of 10 μm thick steel versus repetition rate at constant average power

8.4 Typical Micromachining Conditions and Methods for Up-scaling

8.4.1 Small Aspect Ratio Processes

Microstructuring with ultra-short pulsed laser radiation can be subdivided in small aspect ratio¹ processes and high aspect ratio processes. Small aspect ratio processes like cutting substrate with an aspect ratio 3, thin-films, or free-form texturing need ultra-short pulsed laser radiation with low pulse energies and high repetition rates. Cutting depends on the material properties, the thickness, and the pulse overlap (Fig. 8.5). Thin-films can be removed with ultra-short pulsed laser radiation with little or no pulse overlap, either by ablation (melting and vaporization), or for a substrate transparent for the laser radiation, by chipping the metal from the backside of the substrate, see Fig. 8.6.

An advantage of microstructuring thin-films close to the ablation threshold is precise ablation with little plasma plumes at small electron and ion densities. Therefore, the subsequent laser radiation does not interact significantly with the plasma, and does not induce plasma heating of the surface. This allows an increase of the repetition rate into the multi-100 kHz regime without altering the ablation quality. Nevertheless, care must be taken not to alter the material, because heat induced by the tail of Gaussian shaped radiation is localized in a thin layer.

¹The aspect ratio is defined here as the ratio of the structure lateral size and the structure depth.

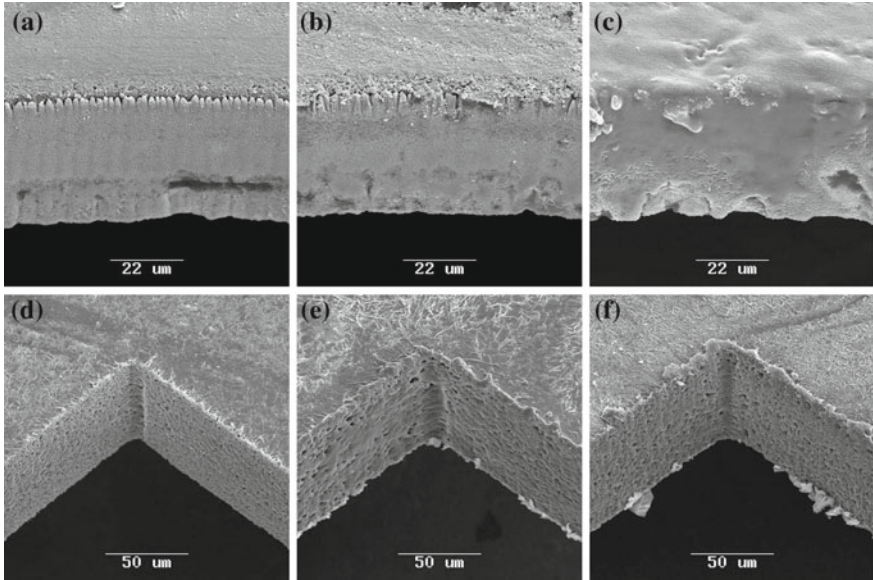


Fig. 8.5 SEM images of cutting edge in silicon (a–c) and Nylon (d–f) produced with a variable pulse overlap (a/d: 55 %, b/e: 75 %, c/f: 95 %) [5]

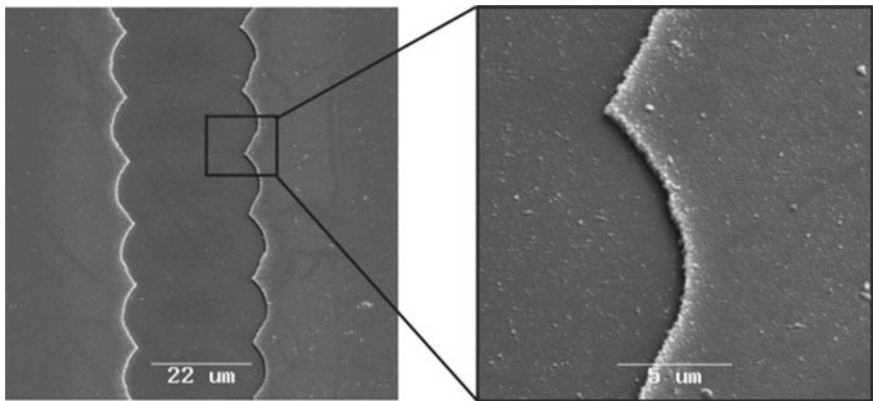


Fig. 8.6 Chipping of thin-film molybdenum (thickness 500 nm) from a glass substrate with little pulse overlap using laser radiation with 600 ps pulse duration [4]

8.4.2 High Aspect Ratio Processes

Contrary to small aspect ratio processing, hole drilling, excavation, or cutting on substrate thicknesses $>250\ \mu\text{m}$ (aspect ratios $\gg 3$) requires high fluencies at moderate repetition rates ($<150\ \text{kHz}$). The repetition rate must be decreased

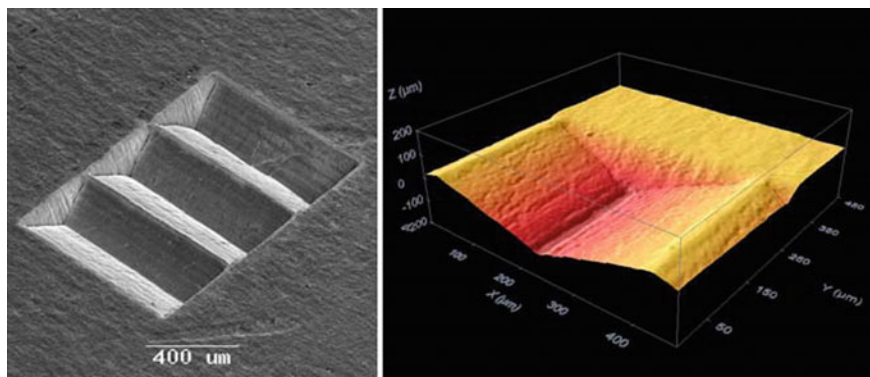


Fig. 8.7 Prism structure in tungsten: SEM (*left*), Laser scanning micrograph (*right*)

significantly to increase fluence, because plasma shielding inhibits laser ablation, and the high energy plasma plume acts as a secondary heat source, negatively altering ablation. Because the optical properties of the material are also altered by ablation, the ablation rate will consequently change, requiring adaption of the fluence during processing. Ablation of multiple layers requires a dynamic adaption of the focal plane.

Removing large amounts of material generates a lot of debris. Depending on the material properties and the laser parameters, the debris adheres to the material surfaces and cannot be removed during laser processing, which further inhibits the ablation process. High-power aspiration on the one hand, and a high-pressure process gas stream on the other hand can avoid the re-deposition of most debris. Complex 3-D structures, for example in tungsten, can then be generated at high aspect ratios (Fig. 8.7), and the material can be removed layer by layer in real-time by adapting the process parameters.

Alternatively a combined process can be developed, first ablating the material with large fluencies to achieve rough structures. Then, high-precision laser structuring at small to moderate fluencies is used to generate acceptable surface qualities with a roughness in the range of the applied wavelength. Thus, the excessive roughness and the heat affected layer are removed.

8.4.3 Limitations

Ultrafast laser processing can be used to very precisely ablate material. However, materials emit surface plasmons during irradiation. The surface plasmons interact coherently with the incoming radiation and change the absorption properties of the surface drastically, e.g. imposing a spatial, periodically varying absorptivity which limits the resolution of micromachining. As a consequence of the changed absorptivity, also the ablation changes by locally generating ripples [10] (Fig. 8.8).

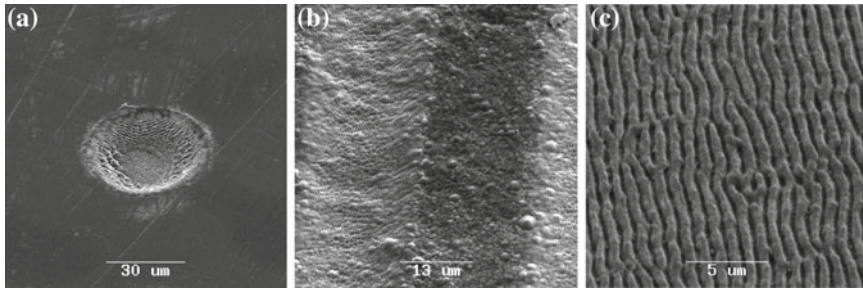


Fig. 8.8 Laser-induced periodic structures (LIPS) **a** in an ablated crater of NiCr film, **b** in linear scribes on polycrystalline diamond, **c** on steel surface

Ripples, also called LIPS (Laser-Induced Periodic Structures) are periodic structures with about the laser wavelength in periodicity, and with an orientation perpendicular to the laser polarization direction. Looking closer at LIPS, two types of ripples are observed, the HF-LIPS and the LF-LIPS [11, 16, 19]. Avoiding ripple formation is still a topic of research. Micro structuring close to the ablation threshold using circular polarized laser radiation might reduce ripple formation. But, because the manipulation of the laser radiation to ideal circularity is a nearly unreachable effort, real circular polarized radiation will even induce ripples itself. Processing with long pulsed laser radiation in the nanosecond regime can smooth the surface by melting the ripples, or chemical etching can be used.

Even processing metals and semiconductors at moderate to high fluencies, $2-5 F_{thr}$ will induce quasi-periodic features, so called cones [10, 17]. The periodicity depends not only on the radiation wavelength, but also on the processing parameters (such as fluence, overlap, focusing diameter, repetition rate, processing gas). Cones are applied for reflectivity reduction in electronics, especially for semiconductor detectors and photovoltaic elements.

8.4.4 Frequency Conversion

Picosecond and femtosecond laser radiation can efficiently be frequency-converted into lower or higher frequency harmonics of the fundamental wavelength with very high power densities. The fundamental wavelength of the laser radiation is typically in the near-infrared regime. Optical equipment such as dielectric mirrors or lenses, and optoelectronic components such as optical switches, nowadays feature industrial standards with high quality, and offer a nearly loss-free transmission or deflection of radiation. Generally, converting laser radiation to higher harmonics can better focus the radiation, e.g. the focal diameter scales with about half the wavelength, and allows micro structuring close and even below diffraction limit.

Diffraction limited infrared ultrafast laser radiation converted by second harmonic generation (SHG) into the visible spectrum features radiation with excellent

beam quality $M^2 \approx 1$, and conversion efficiency as high as 80 %. All available conventional optics for visible radiation can be adopted for micromachining, also allowing the use of microscope lenses for focusing and microstructuring in the micrometer range. Because conventional optics is designed for low intensity radiation, care must be taken not to damage the optics due to overloading. Specially designed high-power optics for ultra-short pulsed laser radiation allow microstructuring at high fluencies.

Microstructuring with ultraviolet laser radiation can be used to “ablate cold” organic materials such as polymers, by photo-chemically breaking the chemical bonds. Converted IR laser radiation into the ultraviolet regime by third harmonics (THG) or fourth harmonics generation (FHG) is applicable today, especially the THG. But due to aging, the lifetime of the converting crystals is limited, and continuous operation on an industrial level (24/7) is not achievable. Conversion efficiency up to 30 % has been reported for THG. Also, the THG beam quality has negative effects on suffers little on the crystal quality, resulting in a non-diffraction limited radiation $M^2 \approx 1.5$. High-power optics for UV converted YAG radiation are available today.

8.4.5 *Scaling Up*

Scaling up of micromachining using ultra-short laser sources is predominantly done by increasing the repetition rate, or by applying multiple beams. However, fast micromachining with all the features of cold ablation limits the maximum repetition rate, since:

- (a) residual heat due to incomplete transfer of absorbed pulse energy into ablation, and
- (b) temporal and spatial overlap of pulse sequences

results in accumulated and residual heat. Apart from scaling up the microstructuring process by increasing fluence (see Sect. 8.2) and repetition rate (see Sect. 8.3) of the laser radiation, a process can be parallelized by multiplying the number of laser beams using conventional beam splitting optics, or diffractive optical elements (DOE). Depending on the application, the multi-beams are either separated, and each of the beams delivered to different machining stations, or the beams are focused on one micromachining station (Fig. 8.9).

A single laser beam can be multiplied using DOEs, increasing the number of beams linearly up to about 100 spots, or distributed on a matrix up to 10×10 beams (Fig. 8.10). The diffraction efficiency is now about 80 % of the incoming radiation. Zero-order diffraction is often implemented in the diffraction scheme.

Speeding-up is achieved by increasing the scanning velocity using high-speed galvano scanners (limited to about 10 m/s at 100 mm focus length), or polygon scanners (limited to 360 m/s at 100 mm focus length). Volumes up to $2 \text{ mm}^3/\text{s}$ are removed using high-power, high-repetition rate ultra-short laser machining systems

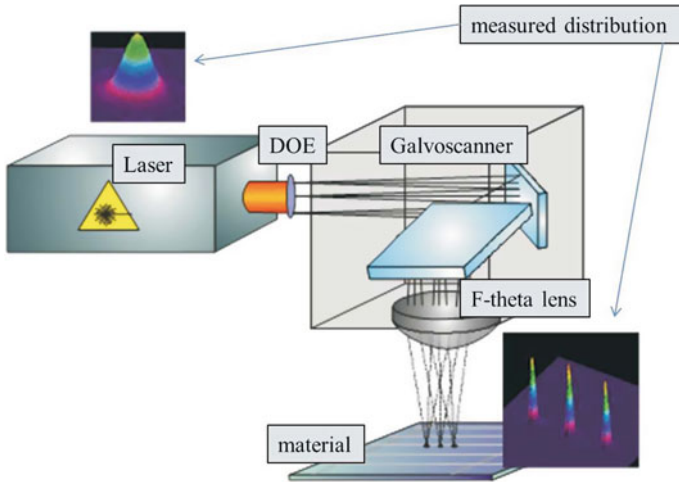


Fig. 8.9 Schematics of multi-beam processing using diffractive optical elements (DOE), scanning technology and focusing optics

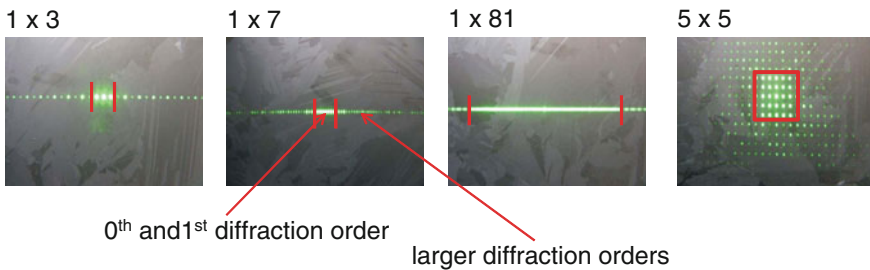


Fig. 8.10 Multi-spot generation using DOE: 3, 7, 81 spots in a line; 5 × 5 matrix, larger diffraction orders outside the red lines contain <5 % of the pulse energy

combining high-speed scanning for one axis, and an electro-optic deflection with low deflection in the other axis. Also, combing a high-speed rotational stage with a slow co-axial axis allows micromachining on the shell of cylindrical samples with high processing velocities.

Spatially shaping the intensity distribution of the focused laser radiation reduces the amount of wasted energy, i.e. energy not used for ablation. For example, micromachining with diffraction-limited laser radiation suffers of the heat load given by the tails of the Gaussian distribution and the ablation threshold (Figs. 8.3 and 8.11). Spatially shaping the laser radiation to achieve a top-hat shaped focused radiation can be used for ablating materials with a reduced heat-affected zone (Fig. 8.11). Exemplary, patterning of molybdenum layers using shaped laser radiation reduces the heat load, and also the pulse overlap.

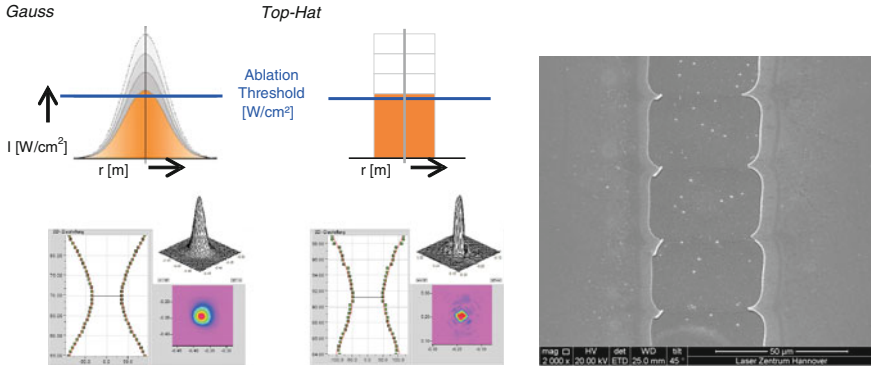


Fig. 8.11 Schematics of diffraction-limited and top-hat distributions (*top*) with defined ablation threshold. Measured caustic and focal intensity distributions (*bottom*). SEM of ablated Mo-layer using top-hat distribution (*right*)

8.5 Exploitation of Residual Heat

Heat accumulation during ultra-short laser micromachining can be successfully applied in different processes: Multi-photon absorption of ultra-short laser radiation can be used to deposit much localized. Heating and melting using high-repetitive laser radiation with repetition rates beyond 100 kHz benefits of heat accumulation [6, 7]. Focusing the radiation at the boundary of two compressed glass plates results in welding glass with little mechanical stress. Moving the laser radiation relative to the substrates generates a welding seam with lateral dimension well below 100 μm , with excellent bonding strengths [12].

Thin-film metals and semiconductors such as ITO (Indium tin oxide) and zinc oxide are adopted for electronics, photovoltaic, and lighting. Their optical and electrical properties often need to be altered after deposition on the substrate. For example, ZnO_2 thin-films exhibit poor optical properties and low electrical conductivity after deposition. Conventional thermal treatment, so called annealing, is achieved by furnace treatment, a slow and expensive process. Using laser radiation optical energy can be localized within the layer, not stressing the substrate. Apart from continuous wave laser treatment, also ultra-short high-repetition laser treatment is applicable. A very precise and spatially localized heat input is used to thermally treat thin layers, preserving thermally sensitive substrates [4].

Conventional laser microstructuring of ceramics induces microcracking because of the excessive heat load. By using ultra-short laser radiation crack-free ablation is possible. The re-depositions generated during multi-pass irradiations of up-scaled ultra-short laser processes, however, firmly adhere to the inner surface of the ablation trench which cannot be removed by compressed air or by ultrasonic cleaning any more. In case of an electromechanic component such as a piezo stack, where a metallic inter layer has to be recessed within the ceramic bulk material

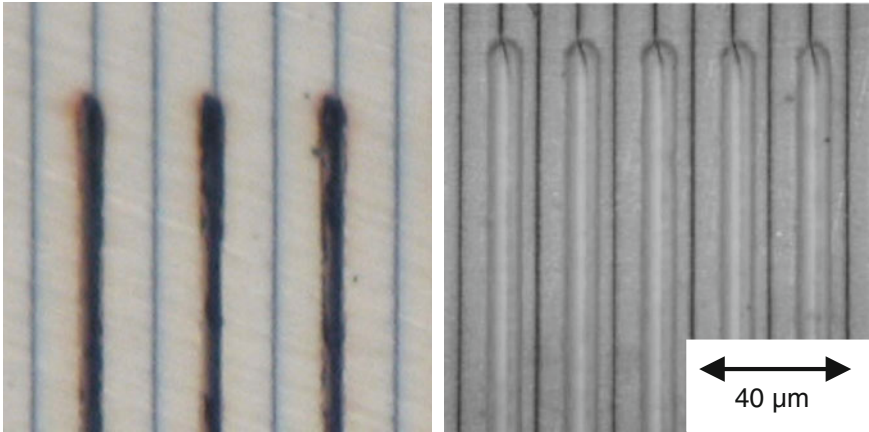


Fig. 8.12 Laser-structured piezo stacks emphasizing “cold” ablation: metallic recast blocks functionality (*left*). Well-balanced laser processing applying residual heat results in recast-free structures on piezo stacks (*right*)

(green part), the metallic re-depositions alter the electric properties of the post-processed (debindered) ceramic (Fig. 8.12 left). In the worst case the piezo stack is then non-functional. A novel process has been developed, applying ultra-short laser radiation with well-balanced laser process parameters, especially pulse energy and repetition rate. Localized heating of the immediate vicinity of the ablation trench results in delayed flaking of the re-depositions by heat induced exudation of the surrounding binder material of the green body. A simple ultrasonic post-treatment completely removes the metallic debris (Fig. 8.12 right).

8.6 Scenarios for the Transfer of Ultra-fast Pulsed Processes to Large Scale Industrial Applications

8.6.1 Electrical Deactivation of Piezo Stacks Using Laser Ablation

Laser microstructuring of piezo stacks for automotive injection modules using ultra-short pulsed laser radiation is investigated here. The aim was to find a way to save costs with a new process, and at the same time to increase the performance and the durability of the product. The piezo stacks consist of a series of piezo ceramics layers (thickness 70 μm) divided by metallic, electric conducting layers (thickness 2 μm). In order to connect two piezo elements in series, the electrical conductor of every second piezo layer has to be removed locally using laser ablation, as shown in Fig. 8.13. Using ultra-short laser radiation, full active stacks were generated with

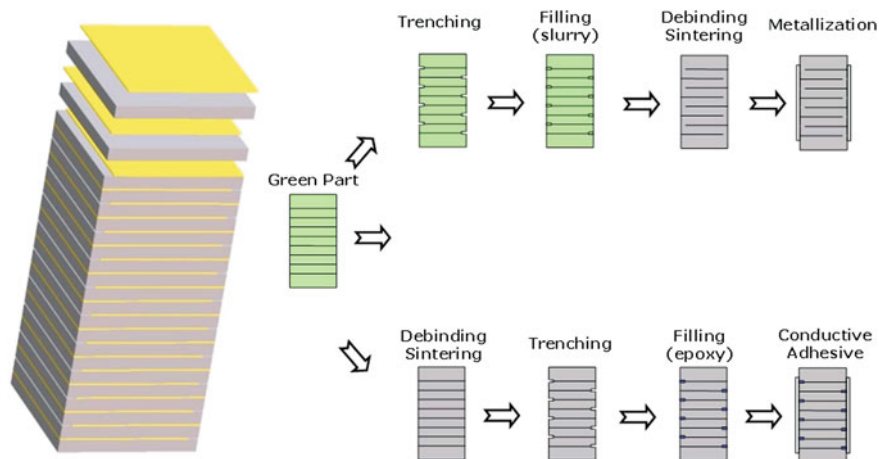


Fig. 8.13 Principle of electrode deactivation (*left*), technological variants for the fabrication of piezoelectric stacks with alternating electrodes (*right*): structuring of *green part* first (*upper scheme*) and first sintering then structuring (*lower scheme*)

reduced micro-cracking. Two strategies for accomplishing electrical isolation have been investigated (Fig. 8.13 right):

1. After sintering the green part (see Fig. 8.13), the electrical isolations of the piezo stack electrodes is achieved by ablating gaps between two piezo cells using “cold” ablation of the metallic layer
2. Using laser structuring, the metallic layer is removed from the green part. Afterwards, the gap is closed with slurry, and the complete piezo stack is sintered.

Non-thermally loaded ceramic results from using “cold” ablation with ultra-short laser radiation at reduced repetition rates smaller than 100 kHz. However, the re-deposited metal on the walls of the gap influences the electrical conductivity of the filling (Fig. 8.14 left) in post-processing. The re-deposited metal could not be removed by post-processing, such as ultrasound cleaning. Electrical isolation could not be achieved.

A functional piezo stack could be achieved by first structuring the green part and locally removing the metallic layer, and afterwards using ultrasound cleaning, filling and sintering. In order to completely and easily remove the re-deposited metals, the heat load during laser processing was balanced, resulting in a cloudy recast with in clean structures (Fig. 8.14 right).

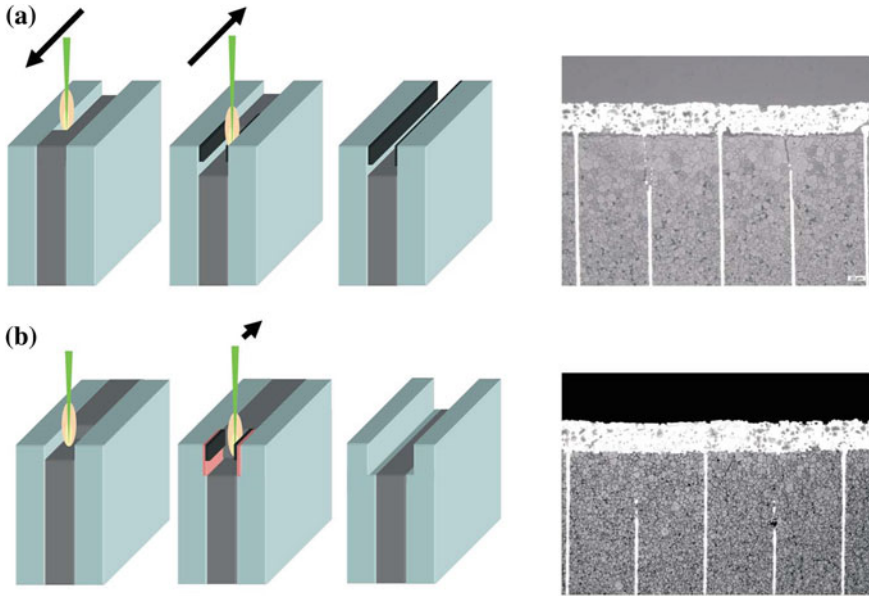


Fig. 8.14 Strategies for gap generation: **a** “Cold” ablation of metallic layer resulting in metallic recast on the walls. **b** Heat accumulated ablation removing metallic layer, and by post-processing the re-deposited material. *Right* SEM of cross-section with piezo-ceramic layers, metallic layer and fillings

8.6.2 Micromachining of Seal Faces Without Post-processing

A leakage trench on a surface of a seal face (Fig. 8.15 left) was accomplished, ablating grooves with a width of about 40 μm and a comparable depth using ultra-short pulsed laser radiation (Fig. 8.15 right). The processing parameters were adapted to form grooves with negligible bulging and recast on the surface. Post-processing of the component was not necessary, reducing production costs.

8.6.3 Efficiency Enhancement by Patterning Si-Solar Cells

The efficiency of multi-crystalline silicon (mc-Si) solar cells can be improved by reducing the amount of reflected solar radiation. Today common techniques are

1. Iso-texture etching for mc-Si,
2. Applying antireflective coatings, and
3. Anisotropic etching for mono-crystalline silicon solar cells for pyramid structures.

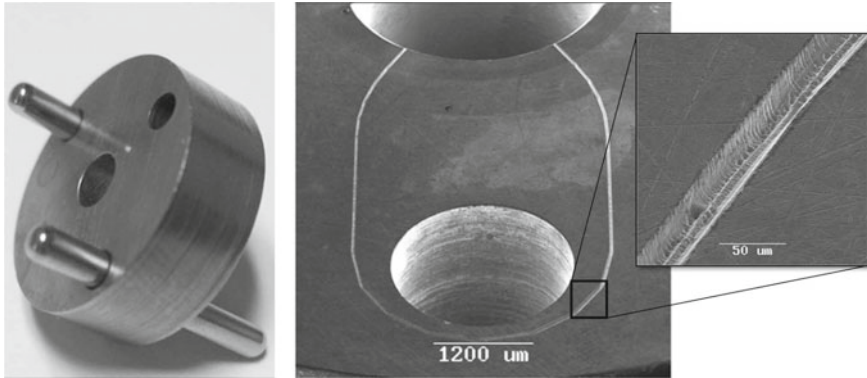


Fig. 8.15 Laser engraved leakage trench on the sealing surface of a buffer (*left*). SEM surface with leakage trench, *inlet* enlargement of leakage trench (*right*)

A reduction of reflectivity using ultra-short laser surface treatment of different materials, including silicon, has already been demonstrated [17].

Here, an alternative approach is shown, which is industrially applicable. High-repetition rate ablation is achieved, by scanning meandrian trajectories with focused laser radiation. By using high-repetition rate laser radiation from an industrial laser in the multi-100 kHz regime, productivity, expressed in m^2/scan , can increase into the productivity range of one 5" wafer per second, at an appropriate mean laser power. Processing is parallelized by using diffractive optical elements to generate multiple laser spots (Sect. 8.4.5) [14].

Depending on the applied fluence, two regimes for ablation are detected (Sect. 8.2). In the optical regime at fluencies below about $4 \text{ J}/\text{cm}^2$, a cone-like topology can be generated, whereas when fluencies are above $4 \text{ J}/\text{cm}^2$, smooth structures attributed to the thermal regime are generated [10, 13]. The surface is modified by ablation, depending on the laser parameters in the optical regime of silicon, by generating cones with sizes of up to $10 \mu\text{m}$ with dimensions in the range of a few μm . The reflectivity is reduced absolutely to about 11 % over the spectral distribution of solar light, in comparison to the standard iso-textured surface on mc-Si solar cells (Fig. 8.16).

8.6.4 3-D Laser Patterning of Thin-Film Strain Sensors

Thin-film strain sensors which are directly deposited onto the surface of mechanical components can be used for measurement of forces, pressure or strain in harsh environments and at high temperatures [18]. Femtosecond laser patterning is used for thin-film sensors on component surfaces. Ultra-short pulsed laser radiation allows high selectivity and quality during ablation of the different thin-film layers

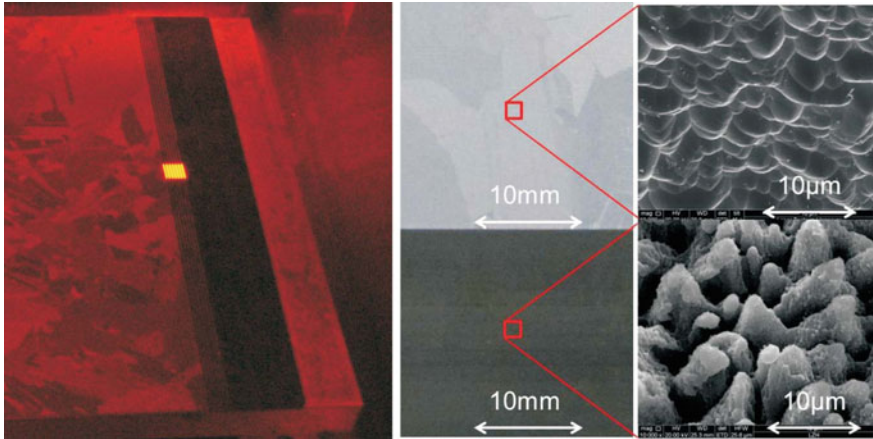


Fig. 8.16 Multi-spot processing of silicon using ultrafast laser radiation (*left*), non-processed, iso-textured silicon surface (*top*) and laser-processed surface (*bottom*)

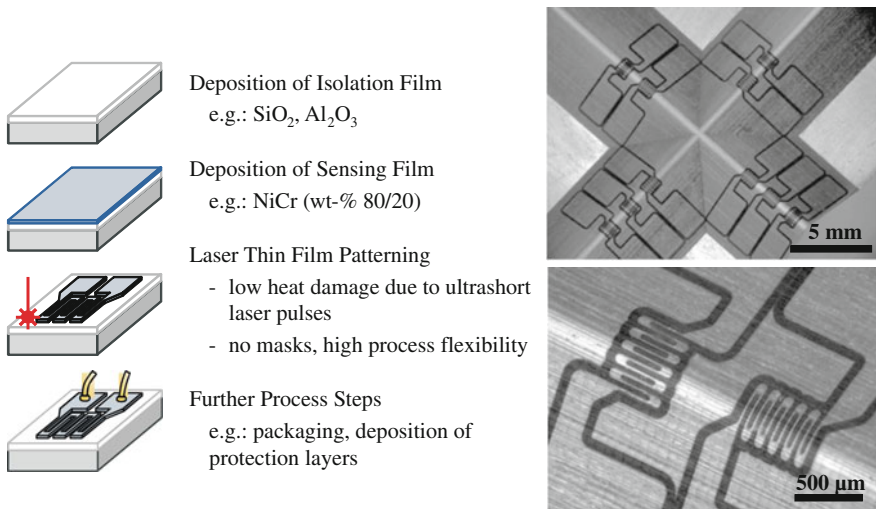


Fig. 8.17 Schematic procedure for laser-processing of thin-film sensors (*left*); laser patterned thin-film strain sensors processed into a *v-shaped* groove of an aluminum component. The top metallic groove of an aluminum component is selectively removed using ultra-short laser pulses (*dark area, right*)

(Fig. 8.17 left). This method is particularly useful for patterning strain sensors which are sputter deposited directly onto curved surfaces.

The ablation behavior of NiCr film irradiated by femtosecond laser pulses at non-normal angles of incidence has been modeled and experimentally verified with linear and circular beam polarization for incidence angles up to 80° [2, 9]. The

ablation threshold behavior can be described when including polarization and angle dependent Fresnel reflection in the laser ablation model. The laser process was demonstrated by patterning NiCr thin-film sensors on the non-planar surface of a mechanical component for a machine tool (Fig. 8.17 right).

8.7 Conclusion

Micromachining using ultra-short pulsed laser ablation is nowadays part of production chains in industry. Today, high-power laser systems in the kW-range are available, with very high repetition rates up to the MHz range, which allow high-quality, highly productive microstructuring of all kind of materials. Due to the unique processes induced by ultra-short laser radiation, on one hand nearly “cold” ablation is achievable, and on the other hand a very precise heat load is applicable for sensitive thermal treatments of materials such as welding of glass and annealing of thin-films.

Acknowledgments This work was supported by German Research Foundation (DFG) within the Collaborative Research Centre CRC 653, “Gentelligent Components in their Lifecycle”.

References

1. B.N. Chichkov Momma, C. Nolte, S. von Alvensleben, A. Tünnermann, Femtosecond, picosecond and nanosecond laser ablation of solids [Article] // *Appl. Phys. A Mater. Sci. Process.* **63**, 109–115 (1996)
2. J.F. Düsing, O. Suttman, J. Koch, U. Stute, Ultrafast laser patterning of thin films on 3-D shaped surfaces for strain sensor applications [Article] // *Proceedings of the 13th International Symposium on Laser Precision Microfabrication (LPM)*, 12–15 June 2012
3. E. Fadeeva, S. Schlie, J. Koch, A. Ngezahayo, B.N. Chichkov, The hydrophobic properties of femtosecond laser fabricated spike structures and their effects on cell proliferation [Article] // *physica status solidi (a)* **206**(6), 1348–1351 (2009)
4. A. Horn C.-C. Kalmbach, J. González Moreno, V. Schütz, U. Stute, L. Overmeyer, Laser-surface-treatment for photovoltaic applications [Article] // *Physics Procedia* **39**, 709–716 (2012)
5. U. Klug, U.B. Kamlage-Rahn, J. Koch, R. Knappe, U. Stute, B. Chichkov, Picosecond laser material processing—prospects and limitations [Article] (2006)
6. I. Miyamoto, K. Cvecek, Y. Okamoto, M. Schmidt, Novel fusion welding technology of glass using ultrashort pulse lasers [Article] // *Physics Procedia* **5A**, 483–493 (2010)
7. I. Miyamoto, A. Horn, J. Gottmann, D. Wortmann, F. Yoshino, Fusion welding of glass using femtosecond laser pulses with high-repetition rates [Article] // *JLM-N J. Laser Micro/Nanoeng.* **2**(1), 57–63 (2007)
8. S. Nolte, C. Momma, H. Jacobs, A. Tünnermann, B.N. Chichkov, B. Wellegehausen, H. Welling, Ablation of metals by ultrashort laser pulses [Article] // *JOSA B.* **14**, 2716–2722 (1997)
9. L. Overmeyer, J.F. Düsing, O. Suttman, U. Stute, Laser patterning of thin film sensors on 3-D surfaces [Article] // *CIRP Annals Manufact. Technol.* **61**(1), 215–218 (2012)

10. L. Overmeyer, V. Schütz, A. Horn, U. Stute, Laser induced quasi-periodical micro-structures with external field modulation for efficient gain in photovoltaics [Article] // *CIRP Annals Manufact. Technol.* ed. Elsevier **62**(1), 207–210 (2013)
11. H. Raether, Surface plasmons on smooth and rough surfaces and on gratings [Book], vol. 111 (Springer, Berlin, 1988)
12. S. Richter, S. Nolte, A. Tünnermann, Ultrashort pulse laser welding—a new approach for high-stability bonding of different glasses [Article] // *Physics Procedia*. **39**, 556–562 (2012)
13. V. Schütz, A. Horn, U. Stute, Investigations into laser edge isolation (LEI) of mc-Si solar cells using ns- and ps-laser radiation [Article] // *Photovoltaics International 14th Ed.* vol. 11, pp. 69–76 (2011)
14. V. Schütz, A. Horn, U. Stute, High-throughput process parallelization for laser surface modification on Si-Solar cells: determination of the process window [Article] // *Proc. SPIE*. **8244**, 33 (2012)
15. F. Siegel, U. Klug, R. Kling, Extensive micro-structuring of metals using picosecond pulses—ablation behavior and industrial relevance [Article] // *JLMN-J. Laser Micro/Nanoeng.* **4**, 104–110 (2009)
16. M. Straub, M. Afshar, D. Feili, H. Seidel, K. König, Surface plasmon polariton model of high-spatial frequency laser-induced periodic surface structure generation in silicon [Article] // *J. Appl. Phys.* **111**, 124315 (2012)
17. B.R. Tull, J.E. Carey, E. Mazur, Silicon surface morphologies after femtosecond laser irradiation [Article] // *MRS Bull.* **31**, 626–633 (2006)
18. G.R. Witt, The electromechanical properties of thin films and the thin film strain gauge [Article] // *Thin Solid Films* **22**, 133–156 (1974)
19. A.I. Zayats, I. Smolyaninov, Near-field photonics: surface plasmon polaritons and localized surface plasmons [Article] // *J. Opt. A: Pure Appl. Opt.* **5**, 16 (2003)